Diffusion of Tracer Molecules within Symmetric Diblock Copolymers

John M. Zielinski,† Gerhard Heuberger, and Hans Sillescu

Institut für Physikalische Chemie der Universität Mainz, Jakob-Welder-Weg 15, 55128 Mainz, Germany

Ulrich Wiesner,* Andreas Heuer, Yuanming Zhang, and Hans W. Spiess

Max-Planck-Institut für Polymerforschung, Postfach 3148, 55021 Mainz, Germany

Received March 17, 1995; Revised Manuscript Received August 14, 1995®

ABSTRACT: Forced Rayleigh scattering has been used to investigate tracer diffusion of a tetrahydrothiophene–indigo derivative (TTI), a photochromic dye molecule, in a macroscopically isotropic lamellar poly(styrene-*b*-isoprene) diblock copolymer of relative high molecular weight. As anticipated from the large difference of segmental mobility between the constituent blocks, three relaxation processes termed fast, intermediate, and slow, respectively, have been observed as a function of temperature and grid spacing for the decay curve of scattered light from the photoinduced grating in the experiments. The fast process exhibits a q^2 dependence, which is characteristic of Fickian diffusion, whereas the slow process is independent of q. Model calculations have identified the nature of these two processes. In addition, the role of the size of the grid spacing chosen in these experiments, relative to the lamellar period of the microstructure, has been elucidated. A means of extracting diffusion coefficients for TTI in PI and PS lamellae from the experimental results has been demonstrated. A comparison of the diffusion coefficients obtained from the PI and PS lamellae in the block copolymer with those of TTI diffusion in PI and PS homopolymers revealed differences in the temperature dependence between the homogeneous and microstructured materials.

Introduction

In recent years the diffusion of tracer molecules and chains in homopolymer melts has been the subject of intense interest. Scaling laws and diffusion behavior in the vicinity of the glass transition temperature T_g could thus be established for a variety of different penetrant structures and chain topologies.[1] In contrast, relatively little is known about mobility in microstructured block copolymers.[2–5] These materials have attracted increasing interest because of their ability to form a surprising variety of ordered equilibrium structures[6–14] that can be strongly influenced by external mechanical fields.[15–17] In these systems, transport properties are particularly interesting since the supramolecular structure imposes spatial constraints on a diffusing moiety which, in special cases, can lead to anisotropic behavior.[18,19]

To investigate the effect of the lamellar morphology on tracer diffusion, forced Rayleigh scattering (FRS), a holographic technique which enables measurement of small diffusion constants[20,21] ($\sim 10^{17}$ cm^2/s), has been employed to investigate diffusion dynamics in nearly symmetric polystyrene (PS)–polyisoprene (PI) A–B type diblock copolymers. In this technique a grating is induced in the sample via interference of two coherent laser beams at an angle θ. The time evolution of this grating is then monitored by a subsequent diffraction experiment. The advantages of this method over other techniques are the high resolution of even small differences in the refractive index, the possibility of measuring precise relaxation times over a wide range ($1-10^5$ s), and good experimental reproducibility. Translational diffusivity is widely accepted as a fundamental quantity reflecting polymer dynamics. Thus, for block copolymers like PS–PI with a large difference in segmental mobility, as signified by a difference in glass transition temperatures of more than 100 K, multicomponent relaxation processes are expected to occur. Such processes could provide a fingerprint of the microphase-separated structure, thereby raising the issue of mobility within the interphase.

In the present work, results for diffusion of the tracer molecule TTI, a tetrahydrothiophene–indigo derivative, in a macroscopically isotropic lamellar PS–PI block copolymer, as measured by FRS, are presented. It is shown that, for these systems, the decay curve of scattered light from the photoinduced grating indeed indicates the existence of several processes. With the help of model calculations the nature of these processes is elucidated, thereby demonstrating that (i) FRS supplies detailed insights into the mechanisms of small-molecule diffusion in block copolymers and (ii) tracer diffusion is a powerful tool for probing the local mobility distributions and microstructure in microphase-separated block copolymers.

Experimental Section

Materials. Polymers. The poly(styrene-*b*-isoprene) diblock copolymer, designated PS–PI-6 in our nomenclature, has been synthesized by living anionic polymerization using cyclohexane as solvent and *sec*-butyllithium as initiator. The PS and PI block molecular weights M_w are 92 400 and 84 000, respectively, as determined by GPC for the PS precursor and ^{13}C NMR for the PI block. The dispersity M_w/M_n as determined by GPC for the block copolymer is 1.06. All GPC analyses were performed using polystyrene as the standard. The uncertainty in the molecular weight is about 5% for both techniques. The T_g's of the PS and PI blocks as determined by DSC at a heating rate of 10 K/min were 373 and 216 K, respectively. The characteristics of the block copolymer are summarized in Table 1, along with corresponding data for PI and PS homopolymers used for comparison in this study. The PI homopolymer was obtained from Polymer Standards Service (PSS), Mainz. Details of the characterization, as well as tracer diffusion data

† Current address: Air Products and Chemicals, Inc., 7201 Hamilton Boulevard, Allentown, PA 18195-1501.

® Abstract published in *Advance ACS Abstracts,* October 15, 1995.

0024-9297/95/2228-8287$09.00/0

Table 1. Characterization of Polymers Used in the Present Study

polym code	wt % of PS	M_w of copolymer	M_w of PS	M_w of PI	dispersity U	T_g (K) PS	T_g (K) PI
PS–PI-6	52	176 400	92 400	84 000	1.06	373	216
PS[a]	100		356 400		1.32	369	
PI				10 800	1.02		210

[a] From ref 22.

for the PS homopolymer, are provided in ref 22. The diblock copolymer diffusion measurements have been performed in the microphase-segregated regime, i.e., below the order–disorder transition temperature, T_{ODT}, which lies far above the decomposition temperature of PS–PI-6 and has therefore not been determined experimentally. Under these conditions the block copolymer exhibits the lamellar morphology (verified by electron microscopy; data not shown). The lamellar period, as determined from the relation given in ref 23 for the dependence of the average domain spacing on molecular weight for symmetric PS–PI diblock copolymers $\lambda = 0.024M_n^{2/3}$ (nm) is $\lambda = 73$ nm. In all of the block copolymer samples, as well as the polyisoprene homopolymer, 2,6-di-*tert*-butyl-4-methylphenol was added as an antioxidant.

Tracer Molecule. TTI, 2,2′-Bis(4,4-dimethylthiolan-3-one), has been employed in our FRS measurements as the photochromic dye. It was synthesized following procedures described in the literature.[24,25] Upon irradiation, it undergoes a trans–cis isomerization, with the cis-isomer being stable up to 430 K (a temperature never reached in the present diffusion experiments). Under the experimental conditions described herein, the diffusion coefficients obtained are those for *trans*-TTI.[22] For more details regarding the photochemistry and stability of TTI in different matrices, the interested reader is referred to refs 22 and 26.

Sample Preparation. The homogeneous PI homopolymer samples were prepared by dissolving a predetermined amount of TTI at room temperature in the viscous PI liquid and annealing the sample for several days at moderate temperatures in a vacuum oven. Diblock copolymer samples were prepared by freeze-drying a benzene solution of the dye and the copolymer, pressing a resulting powder into a pellet, and annealing the pellet for 1–2 days at temperatures 20 K above the PS T_g of the copolymer. The TTI concentration was kept below 0.5 wt % in all experiments to avoid any concentration dependence of the diffusion coefficients (D). In this regime, the measured D corresponds to infinite dilution.[22]

Diffusion Experiments. All FRS measurements employed an Ar ion laser operated at a wavelength L of 488 nm, as described earlier.[1,21,27] Holograms were formed by irradiating light intensities of typically 100 mW/mm^2 for times of about 10 ms. Prior to every experiment, the scattering background, responsible for the incoherent background in the fitting procedure described below, was determined. The first value of the scattering intensity was typically measured 2 s after bleaching. Since the spot size of the laser was only about 1 mm^2, multiple measurements could be made using a single sample.

The temporal scattering intensity, $I(t)$, for a single relaxation process, was analyzed in terms of a Kohlrausch–Williams–Watts function[28] (KWW), being interpreted in terms of a distribution of relaxation times

$$I(t) = \{A \exp[-(t/\tau)^{\beta}] + B\}^2 + C \qquad 0 < \beta \leq 1 \qquad (1)$$

In the case of Fickian diffusion τ^{-1} is given by

$$\tau^{-1} = 4\pi^2 D/d^2 \qquad (2)$$

where the grid spacing, d, is calculated from the angle θ at which the two laser beams intersect the sample

$$d = L/2 \sin(\theta/2) \qquad (3)$$

Experimentally, d can be varied between approximately 0.2 and 100 μm. The parameters A, B, and C determine the amplitude of the signal and the coherent and incoherent backgrounds, respectively. The parameter β characterizes the width of the relaxation time distribution. Multiple relaxation processes were modeled as sums of stretched exponentials. For example, two independent relaxation processes involved in destroying the holographic grating were simulated as

$$I(t) = \{A_1 \exp[-(t/\tau_1)^{\beta_1}] + A_2 \exp[-(t/\tau_2)^{\beta_2}] + B\}^2 + C \qquad 0 < \beta_1, \beta_2 \leq 1 \qquad (4)$$

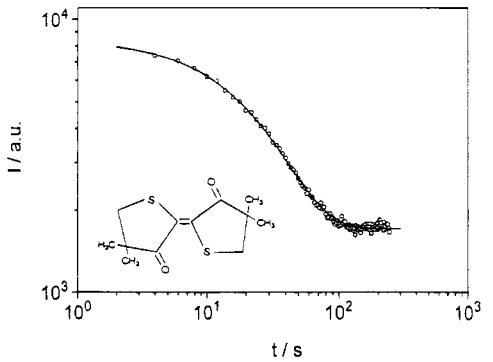

Figure 1. Typical decay curve of the FRS scattering intensity for TTI in the PI homopolymer at temperatures above T_g. Bleaching conditions: 100 mW/mm^2 for 10 ms; $T = 256$ K, $d = 6.2$ μm. The solid line is a fit to a single exponential function according to eq 1. The fit parameters are $A = 82.1$, $\tau = 50.2$ s, $\beta = 1$, $B = 0$, $C = 1700$. The parameter $B = 0$ signifies that the photoinduced grating is completely destroyed by the diffusion process, as expected for polymer melts. These media do not show the long-time stability that would be necessary for optical information storage devices. The chemical formula of the diffusing species, *trans*-TTI, is shown in the inset.

Results

A typical FRS decay curve is presented on double-logarithmic axes in Figure 1 for TTI diffusion in the polyisoprene homopolymer at temperatures above T_g. The double-logarithmic representation of the data is particularly useful in cases where the measurements extend over several orders of magnitude in time and intensity as well as in cases where several processes have to be distinguished (see below). For this homopolymer melt the scattering intensity decays monoexponentially ($\beta = 1$) to the value of the incoherent background measured prior to each experiment independent of the grid spacing d. To guarantee that the process leading to grating destruction is diffusive in nature, the q dependence ($q = 2\pi/d$) of this process has been studied. As expected for Fickian diffusion, the relaxation time, τ, varied quadratically with d (not shown here), thereby leading to a single, well-defined diffusion coefficient.

The decay curves of the FRS signal intensity differ dramatically for the block copolymer. Representative decay curves for PS–PI-6 obtained at temperatures between the two T_g's of the polymer are shown in Figure 2 for two substantially different grid spacings. Figure 2a shows the result of a transmission geometry measurement leading to rather large grid spacings, typically of the order of several tens of micrometers, whereas Figure 2b illustrates the decay curve of a measurement

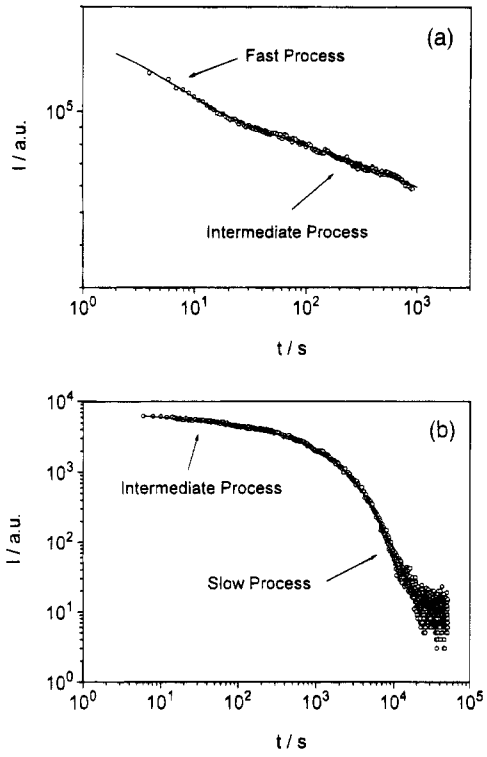

Figure 2. Typical decay curves obtained for TTI in the block copolymer PS–PI-6 at temperatures between the T_g's of the two blocks for two different grid spacings: (a) $d = 66.7$ μm; (b) $d = 0.2$ μm. Bleaching conditions: 100 mW/mm^2 for 10 ms; $T = 350$ K. The solid lines represent fits to a sum of a single exponential and a stretched exponential function. For simplicity in the present study only the relaxation times obtained for the fast and the slow relaxation process that can already be roughly estimated just by looking at the data will be discussed in the text. The analysis of the intermediate process, however, has been omitted since it is difficult to separate the different contributions (see text).

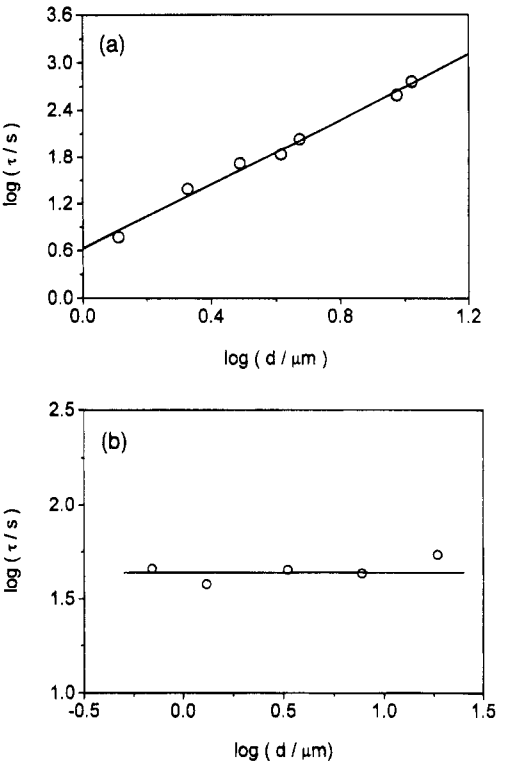

Figure 3. q dependence of the (a) fast and (b) slow relaxation process for PS–PI-6 as a plot of τ obtained from the fits with a single exponential function versus d ($q = 2\pi/d$) used in the experiments. Results from two to three measurements have been averaged to obtain each point. Bleaching conditions: 100 mW/mm^2 for 10 ms; $T =$ (a) 255 K and (b) 376 K. The straight line in (a) is a least-squares fit to the data, exhibiting a slope of 2, as expected for Fickian diffusion. In (b) the straight line exhibits a slope of zero, revealing that the process is q-independent.

obtained in reflection geometry with grid spacings of the order of several hundreds of nanometers only.[1,21] It is important to realize that even for the reflection measurements, the grid spacing is larger than the long period of the block copolymer microstructure. By variation of the grid spacing, as indicated in this figure, three different processes can be observed, which will hereafter be referred to as fast, intermediate, and slow.

In order to discern whether these processes are single-exponential or multiexponential in nature, fits were performed using a sum of two stretched exponentials (see eq 4). Since the exponents for the functions describing the fast and slow process, i.e., either β_1 or β_2, were always close to unity, the data were analyzed in terms of the sum of a single plus a stretched exponential function. The remaining β exponent describing the intermediate process assumed values between 0.1 and 0.3, which corresponds to a very broad distribution of relaxation times.

Since only the fast and slow processes are easy to access in their complete time behavior, in the following section we concentrate our experimental analysis on them exclusively. As in the case of the homopolymer PI, we have analyzed the q dependence for both processes. All measurements have been performed in transmission, leading to grid spacings at least 1 order of magnitude larger than the long period of the block copolymer microstructure. In order to retain readily accessible measuring times, the temperature has been appropriately chosen in each case. For the fast process, the results shown in Figure 3a correspond to a temperature of 255 K, which is about 40 K above the T_g of the PI blocks but well below the T_g of the PS blocks. A least-squares fit of the data reveals that the process exhibits a q^2 dependence. The same analysis for the slow process at 376 K, which is slightly above the T_g of PS, leads to a completely different result. As shown in Figure 3b, the process appears to be independent of q in the examined q range. Following this analysis, the fast process is believed diffusive in nature whereas the slow mode is a local process on the length scale of the grid spacing under these conditions.

Theory of Tracer Diffusion in Lamellar Block Copolymers

In this section we present a theoretical analysis of the complex relaxation patterns observed in the FRS experiments on this two-component system, which involves both q^2- and q^0 dependent processes. Two important features characterize our system. First, for transmission measurements the grid spacing d is orders of magnitude larger than the long period λ of the block copolymer. Second, the fast diffusion coefficient D_f of TTI in PI is expected to be orders of magnitude larger than the slow diffusion coefficient D_S of TTI in PS due to the large difference in T_g of both polymers (see Table 1). Intuitively, one might presume that the condition $d \gg \lambda$ leads to an averaging of the two diffusion coefficients and, hence, to a monoexponential relaxation process since a tracer molecule may jump several times between PI and PS lamellae before moving a distance

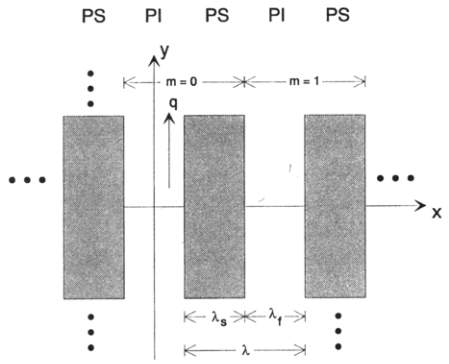

Figure 4. Schematic representation of the block copolymer microstructure with unit normal of the lamellae parallel to the x-axis and q vector of the grid parallel to the y-axis. Dots indicate that the microstructure is infinitely extended. The symbols used here are explained in the text.

of the order d. However, we will see that for $D_f \gg D_s$ even under the condition $d \gg \lambda$, the appearance of several relaxation modes in the FRS experiment can be understood.

For the sake of clarity, the geometry of the block copolymer and one possible grid orientation with respect to the microstructure is illustrated in Figure 4. For simplicity the microstructure is assumed to extend infinitely; i.e. the lamellar extension is much larger than the grid spacing defined by q. Whereas the unit normal of the lamellae is parallel to the x-axis, q has been chosen parallel to the y-axis so that only diffusion in the y-direction leads to a destruction of the grating. It is this orientation of the grid with respect to the microstructure which governs the diffusion behavior. The effect of other orientations is small and will be discussed below. In what follows we present a more phenomenological analysis which allows us to explain the essential features of the relaxation processes observed. For a mathematical exact derivation of the results, the interested reader is referred to the Appendix. For simplicity we assume for the moment that the interface between both polymers is infinitesimally small. We denote the fraction of the two polymers by p_f and p_s and the corresponding widths of the lamellae by λ_f and λ_s ($\lambda_f + \lambda_s = \lambda$). For symmetric block copolymers and the absence of specific interactions we have $p_f = p_s = 1/2$. In general, one has to distinguish two q regimes. In the first regime, in the limit of extremely large grid spacings ($q \to 0$), equilibration of diffusion along the x-direction will always be more efficient than the destruction of the grid. This implies that the relaxation process is identical to that of a homopolymer with averaged diffusion coefficient $\langle D \rangle = p_f D_f + p_s D_s$. In order to deduce the values of q corresponding to this limit, one must estimate the equilibration time t_e along the x-direction. The essential feature of this equilibration process is that tracer molecules in the fast phase (PI lamellae) enter the slow phase with the same rate as molecules from the slow phase enter the fast phase. Violation of this principle would result in an enrichment of the number of TTI molecules in the slow phase. It follows that t_e is determined by the diffusion coefficient D_s and the thickness λ_s of the slow component. In order to estimate t_e, we assume that all tracer molecules are placed in the center of the slow phase and define t_e as the time when, on average, the molecules just reach the boundary. This condition can be approximately written as

$$(\lambda_s/2)^2 \approx 2D_s t_e \tag{5}$$

From eq 2 the time t_q which determines the destruction of the grid in the limit $q \to 0$ is given by

$$t_q^{-1} = q^2 \langle D \rangle \tag{6}$$

The averaged diffusion coefficient $\langle D \rangle$ (see above) and hence a single relaxation time should be observed if the equilibration time t_e is significantly shorter than the time t_q during which the grid is destroyed. For symmetric diblock copolymers, from eqs 5 and 6 this condition is equivalent to

$$((q\lambda_s)^2 D_f)/(16 D_s) \ll 1 \tag{7}$$

In deriving eq 7, we assume $p_f = p_s = 1/2$ and $D_s \ll D_f$. Since the diffusion coefficients of PI and PS differ by at least 9 orders of magnitude, as will be shown later, this limit has not been reached in the present experiments where $q\lambda = 10, ..., 10^{-3}$. In this regime, therefore, we always have $t_e \gg t_q$.

In the q regime for which $t_e \gg t_q$ the slow phase, i.e. the PS lamellae, can effectively be considered as impenetrable walls on the time scale during which the grid of the fast phase is destroyed. Hence, as observed experimentally, the first relaxation process has a relaxation time t_f given by

$$t_f^{-1} = D_f q^2 \tag{8}$$

as expected for Fickian diffusion and the information about the diffusion coefficient D_f of TTI in PI can, as shown earlier, be readily extracted from FRS data in the common way. Of course, the relative amplitude of this process has to be p_f.

The second distinct relaxation process at long time is related to the destruction of the grid in the slow phase. In principle this can occur in two different ways. First, a tracer molecule may stay in the slow phase until it has moved a distance d in the y-direction. This would correspond to Fickian diffusion with $t_s^{-1} = D_s q^2$. However, in the limit $d \gg \lambda_s$, this process is very unlikely to be observed. Rather, the molecule will most probably enter the fast phase before moving a significant distance relative to d in the y-direction. Reentrances into the slow phase are presumed unlikely since, on average, the molecule will stay in the fast phase for a time t_e which is much longer than t_f. Therefore this process leads to a destruction of the grid on the time scale of t_e, as determined by the time the molecule initially stayed in the slow phase. Adding both rates together, one may estimate the relaxation time t_s of the slow relaxation process observed in the experiments by

$$\begin{aligned} t_s^{-1} &= D_s q^2 + t_e^{-1} \\ &= D_s(q^2 + 8/\lambda_s^2) \end{aligned} \tag{9}$$

If the grid spacing d is much larger than the width of the lamellae of the slow phase, the second term dominates the relaxation time and hence the process is independent of q, in agreement with the experimental results depicted in Figure 3b.

The derivation of eq 9 is only qualitative. One possible problem that needs to be addressed is that the time a particle needs to leave the slow phase strongly depends on its initial position. This complication might

smear out the final relaxation process. Therefore it is essential for a quantitative analysis of the FRS data to derive eq 9 from first principles and check whether the final relaxation process is well described. A more rigorous derivation of eq 9 is presented in the Appendix. It is based on the determination of the eigenvalues of the underlying differential equation. There we show that, in the limit $t_e \gg t_q$, the longest relaxation time t_s observed experimentally can be written as

$$t_s^{-1} = D_s(q^2 + \pi^2/\lambda_s^2) \tag{10}$$

which apart from a slightly different numerical factor is indeed the same as eq 9. Furthermore we show that there are additional processes from tracer molecules initially close to the boundary of the slow phase with relaxation times between t_s and t_f. While these relaxation times contribute to the intermediate regime, they only mildly influence the long-time properties. Therefore, the final relaxation is well-defined and can be described by a single exponential. The functional form describing the intermediate regime is also calculated in the Appendix and could thus be used for a quantitative analysis of the experimental results. In real systems, however, one must take into account the interface, which gives rise to additional processes between the fast and the slow limit. The calculation of interfacial contributions is beyond the scope of this paper and we have therefore omitted the analysis of this process.

In our previous analysis we have considered only one orientation of the grid with respect to the microstructure where the unit normal of the lamellae lay along x while q was parallel to the y-axis. The effect of orientation on molecular diffusion within a lamellar phase with impenetrable walls is, however, a standard diffusion problem. In fact, averaging over all possible orientations yields a mean tortuosity factor of $^2/_3$ for the diffusion coefficient D_f.[29] Since the time constant of the slow process is determined by the time a molecule requires to exit a PS lamella, the observed diffusion coefficient, D_s, is independent of orientation. The only exception is the case where q is parallel to the unit normal of the lamellae for which the molecule has to diffuse through many lamellae in order to destroy the grating. This orientation, however, has a very low statistical weight and can, therefore, be neglected.

Discussion

From the results of the previous section, it follows, that the fast and slow processes observed in our FRS experiment can be quantitatively analyzed in terms of diffusion coefficients for TTI diffusion in PI and PS lamellae using eqs 8 and 10, respectively. Thus, employing relaxation times regressed for these processes, diffusion coefficients have been calculated for measurements at varying temperatures above the glass transition of the PI blocks. For each temperature, results of at least two to three measurements have been averaged. The resulting diffusion coefficients are depicted as an Arrhenius-type diagram in Figure 5. In addition, our temperature-dependent data of TTI diffusion in the PI homopolymer and results for a PS homopolymer of relatively high molecular weight are included for comparison.[22] The latter show the typical departure of tracer diffusion coefficients from Williams–Landel–Ferry behavior[30] (WLF) observed for temperatures below the glass-transition temperature T_g.[22] The lines through the homopolymer data correspond to regression

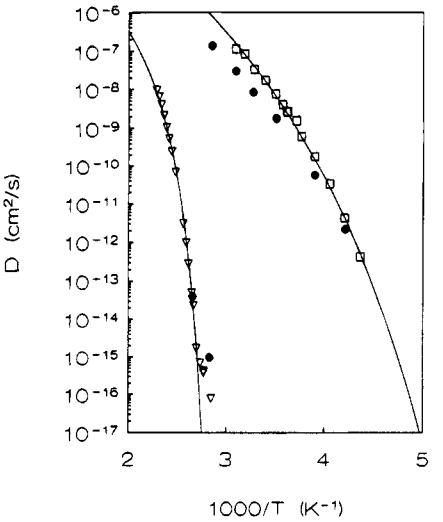

Figure 5. Arrhenius plot of the diffusion coefficients obtained for TTI in PS–PI-6 (●). For comparison, the diffusion coefficients of TTI in PI (□) and PS[22] (▽) homopolymers are also included. The lines through the homopolymer data correspond to the WLF relationships with C_{1g} and C_{2g} values of 13 and 72.1 K for PI and 13.7 and 46.2 K for PS. Furthermore, coupling parameter values (ξ) of 1.06 and 0.75 and $D(T_g)$ values of 6.48×10^{-16} and 6.93×10^{-15} cm^2 s^{-1} were used for PI and PS, respectively (see eq 11).

fits using the WLF relationship for low solute concentrations at temperatures above T_g, as formulated by Fujita[31] and elaborated further by Vrentas et al.[32–35]

$$\log \frac{D(T)}{D(T_g)} = \frac{C'_{1g}(T - T_g)}{C_{2g} + T - T_g} \tag{11}$$

Here C'_{1g} is related to the corresponding WLF parameter of the matrix via the coupling parameter ξ:

$$C'_{1g} = \xi C_{1g} \tag{12}$$

The corresponding fit parameters are provided in the figure caption.

Whereas the fast process was studied over a broad temperature range (233–350 K) above the T_g of PI, diffusion coefficients for TTI in the PS blocks could only be measured for two different temperatures near the T_g of PS (373 K). At 376 K, the slow mode has a relaxation time τ of about 40 s (see Figure 3b). A significant temperature increase will shift τ to much smaller times, which cannot be observed with our present experimental apparatus. Since the process is independent of q at these temperatures, an increase in the grid spacings usually employed in the case of Fickian diffusion does not increase the relaxation time. On the other hand, as depicted in Figure 2 for 350 K, lower temperatures render the relaxation times of the slow process exceedingly long due to the steepness of the temperature dependence in this range, as evident from the PS homopolymer data. Thus, only a limited temperature range is accessible experimentally and the two measurements serve as representative cases.

From Figure 5, diffusion coefficients for TTI in PI and PS homopolymers serve as lower and upper bounds to the fast and slow process, respectively. At 350 K, which is between the two T_g's of the block copolymer, the diffusion coefficients corresponding to these two processes differ by almost 9 orders of magnitude, reflecting the tremendous mobility difference between the PI and PS blocks. These results reveal that tracer diffusion is

a powerful tool for probing the local mobility differences within the microphase-separated structure at the nanometer size scale.

The agreement of the diffusion coefficients obtained for the slow process with the PS homopolymer data is good if one takes into account that, for the measurement below the PS T_g, no special care has been taken with regard to the thermal history of the sample. It is known, however, that physical aging can lead to significant differences in diffusion coefficients within this temperature regime.[22]

The diffusion coefficients for TTI obtained for the fast process are very similar at lower temperatures to those in the PI homopolymer but deviate with increasing temperature. Obviously, the temperature dependence of the two processes is different. To interpret this behavior, it is important to notice that for a q^2-dependent process with increasing temperature, the grid spacings used in the measurements are increased in order to restrict the relaxation times, τ, to an experimentally observable range. As mentioned earlier, d is of the order of several hundreds of nanometers at the lowest temperatures whereas at higher temperatures it is of the order of tens of microns. Thus, the distances over which the TTI molecule must diffuse to eliminate the grating significantly increase with increasing temperature. Under these conditions, the limit of infinitely parallel lamellae is no longer fulfilled (see above). It is not very surprising, therefore, that the temperature dependence of TTI diffusion within a microstructured material, characterized by tremendous mobility gradients and local order, is different than that within a homogeneous medium. From dynamic mechanical measurements, PS–PI block copolymers and related systems are not thermorheologically simple, in which case the WLF-type temperature dependence is not expected to best describe their behavior.[36,37] More experimental work including other techniques like solid state NMR designed to quantify these effects and q-dependent measurements on PS–PI block copolymers of different molecular weights are now in progress in our laboratory.

Finally, we note that the amplitudes of the first process are significantly smaller than 0.5, as expected for large symmetric block copolymers like PS–PI-6. This may reflect a difference of TTI solubility in PS and PI.

Conclusions

We have demonstrated that forced Rayleigh scattering can be used to supply detailed information about the diffusion behavior of small tracer molecules in a lamellar poly(styrene-*b*-isoprene) diblock copolymer which is not directly obtained with integral methods like permeability or sorption measurements.[38–40] As anticipated for such materials with a large difference in segmental mobility between blocks, three relaxation processes termed fast, intermediate, and slow, respectively, have been observed as a function of temperature and grid spacing. With the help of a model calculation, the nature of the fast and slow processes has been identified, and the role of the size of the grid spacing chosen in the experiments with respect to the lamellar period of the microstructure has been elucidated. A method by which to extract diffusion coefficients for tracer diffusion of TTI in PI and PS lamellae from experimental FRS data is proposed. A comparison of the diffusion coefficients obtained for the block copolymer with those of TTI diffusion in PS and PI homopolymers reveals differences in the temperature dependence between the homogeneous and microstructured materials. These differences are the subject of further investigation now in progress in our laboratory.

Acknowledgment. The authors are grateful to A. Doerk for the synthesis of the dye molecule TTI. We thank T. Wagner and T. Volkmer for their help in sample preparation. J.M.Z. gratefully acknowledges financial support provided by the Alexander von Humboldt Stiftung and for partial funding through NSF Grant INT-9201234, while Y.Z. thanks the Volkswagen Stiftung for a stipend.

Appendix

Following the geometry as shown in Figure 4, we assume an infinitely extended microstructure with unit normal of the lamellae along x and q along the y-axis. Since it governs the observed relaxation behavior in the FRS experiments, only this orientation of the grid with respect to the microstructure is taken into account. In this Appendix we will set up the diffusion equation which describes the decay of the grid with time and present an analytical solution of this equation.

At time $t = 0$ the intensity of the grid $g(x,y,t)$ may be written as

$$g(x,y,t=0) = (1/\lambda)\cos(qy) \tag{A1}$$

The time dependence of $g(x,y,t)$ is governed by the two-dimensional diffusion equation

$$\frac{\partial}{\partial t}g(x,y,t) = \frac{\partial}{\partial x}D(x)\frac{\partial}{\partial x}g(x,y,t) + D(x)\frac{\partial^2}{\partial y^2}g(x,y,t) \tag{A2}$$

where $D(x)$ denotes the x-dependent diffusion coefficient. The harmonic concentration profile along the y-direction does not change except for an amplitude which may depend on x and t. Hence we may write

$$g(x,y,t) = h(x,t)\cos(qy) \tag{A3}$$

For the x dependence we expect that the decay of the initial grid intensity $(1/\lambda)\cos(qy)$ is faster in the PI phase than in the PS phase. From eq A2 it follows that the time dependence of $h(x,t)$ is determined by the differential equation

$$\frac{\partial}{\partial t}h(x,t) = -q^2D(x)\,h(x,t) + \frac{\partial}{\partial x}D(x)\frac{\partial}{\partial x}h(x,t) \tag{A4}$$

with the initial condition $h(x,t=0) = 1/\lambda$. Defining

$$H(t) \equiv \int \mathrm{d}x\, h(x,t) \tag{A5}$$

the experimentally observed intensity is proportional to $H(t)^2$ with $H(t=0) = 1$. We have chosen the initial condition such that the initial intensity is 1 if one integrates over one period of the system. Together with the periodicity condition $h(x,t) = h(x+m\lambda,t)$ $(m \in \mathbf{Z})$, eq A4 is a Sturm–Liouville eigenvalue problem.[41]

Furthermore, for symmetry reasons, we have $h(x,t) = h(-x,t)$. The eigenfunctions of the fast phase can either be written as $\cos(k_f(x - m\lambda))$ or $\cosh(k_f(x - m\lambda))$ (in lamella m), whereas those of the slow phase are either $\cos(k_s(x - m\lambda/2))$ or $\cosh(k_s(x - m\lambda/2))$. Since the shape of the eigenfunctions has already been adjusted to the symmetry of our problem, we can restrict ourselves to the case of $m = 0$. The eigenvalue K of the right side of eq A4 is given by

$$K = D_f(\pm k_f^2 - q^2) = D_s(\pm k_s^2 - q^2) \qquad \text{(A6)}$$

The minus sign holds for the cosine functions, respectively. Our goal is to determine all eigenvalues K_n and the corresponding amplitudes A_n such that

$$H(t) = \sum A_n \exp(K_n t) \qquad \text{(A7)}$$

Let $F(x)$ be an eigenfunction which is composed of $F_f(x)$ in the fast phase and $F_s(x)$ in the slow phase. For physical reasons, we know that the grid cannot be destroyed faster than at a rate of $D_f q^2$. Hence, the only relevant combination of eigenfunctions which may fulfill eq A6 with $K < 0$ is $F_f(x) = \cosh(k_f x)$ and $F_s(x) = \cos(k_s(x - \lambda/2))$. The eigenfunctions must satisfy the boundary conditions

$$F_s(\lambda_f/2) = F_f(\lambda_f/2) \qquad \text{(A8)}$$

and

$$D_s \frac{\partial}{\partial x} F_s(x=\lambda_f/2) = D_f \frac{\partial}{\partial x} F_f(x=\lambda_f/2) \qquad \text{(A9)}$$

Dividing eq A9 by eq A8 and specification of the eigenfunctions finally yield

$$D_f k_f \tanh(k_f \lambda_f/2) = D_s k_s \tan(k_s \lambda_s/2) \qquad \text{(A10)}$$

The task is to determine pairs (k_f, k_s) which simultaneously satisfy eqs A6 and A10. The relative amplitude of F_f to F_s can be determined by the continuity condition in eq A8. Note that the value of $\tan(k_s\lambda_s/2)$ is always positive in order to fulfill eq A10. Since eq A10 is a transcendental equation, it is not possible to find a direct solution. However, we will show that solutions can be found in special limits.

We proceed by combining eqs A6 and A10, which yields

$$A^2 = x^2[1 + \tan(x)/(cx)] \qquad \text{(A11)}$$

with

$$A^2 = (q\lambda_s/2)^2(D_f/D_s - 1) \approx (2/p_f)(t_e/t_q) \qquad \text{(A12)}$$

$$x = k_s\lambda_s/2 \qquad \text{(A13)}$$

and

$$c = \lambda_f/\lambda_s \qquad \text{(A14)}$$

For reasons of simplicity, we used the approximation $\tanh(\lambda_f k_f/2) \approx \lambda_f k_f/2$ (equivalently, $\lambda_f k_f \ll 1$). For the cases in which this approximation does not hold, we will show that our results do not change. Equation A11 shows that we were able to decouple the nonlinear set of equations for k_f and k_s. Now we must determine values of x which fulfill eq A11.

In the limit of $A \ll 1$, eq A11 has only a single solution given by

$$x^2 = A^2/(1 + c^{-1}) \qquad \text{(A15)}$$

Since $x \ll 1$, it follows from eq A10 that $k_f\lambda_f \ll 1$. Inserting the corresponding value of k_s in eq A6 one recovers eq 6 after some algebraic manipulations. In agreement with our qualitative derivation in the text the limit $A \ll 1$ or, equivalently, $t_e \ll t_q$, describes the limit in which only a single averaged diffusion constant can be observed.

We now focus on the opposite limit, namely, $A \gg 1$. Due to the unlimited range of values of $\tan(x)$ there exists a solution x_n of eq A11 in every interval $[n\pi, (n + 1/2)\pi]$ $(n = 0, ..., N)$. The largest solution x_N is approximately given by A. Since $A \gg 1$, deviations due to possibly large values of $\tan(x_N)$ can be neglected. Inserting this solution in eq A6, we obtain for the eigenvalue $K_N = -D_f q^2$, which describes the initial relaxation of the fast phase. Again we have $k_f\lambda_f \ll 1$. It can be easily checked that the eigenvalues $-K_n$ with $n \approx N$ are similar to $D_f q^2$ and hence contribute to the initial relaxation. Deviations of the eigenvalues are of the order of $A^{-1/2}$ and hence can be neglected. For physical reasons, the sum over all A_n with $n \approx N$ equals p_f since in the limit $D_s \to 0$ (and hence $A \to \infty$) $H(t)$ is trivially given by $p_f \exp(-D_f q^2 t) + p_s$. The small variation in relaxation times implies the possibility that the tracer molecules leave the fast phase before moving by a distance d in the y-direction.

A very different scenario is related to the solutions with small values of n. In this case eq A11 can only be solved for extremely large values of $\tan(x_n)$, hence $x_n \approx (n + 1/2)\pi$. This corresponds to

$$K_n = -D_s q^2 - D_s \pi^2 (2n + 1)^2/\lambda_s^2 \qquad \text{(A16)}$$

which in the case of $n = 0$ is equal to eq 10 in the text. Hence we already see that the second slowest relaxation mode is already approximately 9 times faster than the slowest mode. The assumption $k_f\lambda_f \ll 1$ does not have to be fulfilled in this limit. Since one always has $\tanh(k_f\lambda_f/2) \geq k_f\lambda_f/2$, additional terms in the series for the tanh function increase the value of A. However, since the x_n do not depend on A (in the limit $A \gg 1$), the results are not changed by including the additional terms.

It is also important to analyze the amplitudes A_n in order to check whether the final relaxation can be well described by a single exponential. It is easy to derive from the continuity condition eq A7 that for $x_n \approx (n + 1/2)\pi$, the eigenfunction in the fast phase can be well approximated by zero. The normalized eigenfunctions $F_{s,n}(x)$ in the slow regime are given by

$$F_{s,n}(x) = (2/\lambda_s)^{1/2} \cos(k_{s,n}(x - \lambda/2)) \qquad \text{(A17)}$$

and the amplitudes A_n can be calculated via

$$A_n = \int dx\, dx'\, F_n(x)\, h(x,t=0)\, F_n(x') \qquad \text{(A18)}$$

For small values of n, eq A18 reduces to

$$A_n = 8p_s/[\pi^2(2n + 1)^2] \qquad \text{(A19)}$$

We see that the sum of the amplitudes for $n > 0$ is only approximately 20% of A_0. Therefore the final process can be well described by a single exponential. Note that $\sum A_n = p_s$, as expected intuitively. Interestingly, it turns out that the relaxation rates $(-K_n)$ as well as the amplitudes (A_n) are identical to the predictions of the short-time dynamics of polymers in the framework of the Rouse model.[42]

In summary, we have determined the time dependence of $H(t)$ in the limiting cases of $A \ll 1$ and $A \gg 1$, yielding

$$H(t) = \exp(-q^2\langle D\rangle t) \qquad A \ll 1$$

$$H(t) = p_f \exp(-q^2 D_f t) + p_s \sum \frac{8}{\pi^2(2n+1)^2} \times \exp[-D_s t(q^2 + \pi^2(2n+1)^2/\lambda_s{}^2)] \qquad A \gg 1 \quad \text{(A20)}$$

References and Notes

(1) Sillescu, H. In *Chemistry and Physics of Macromolecules*; Fischer, E. W., Schulz, R. C., Sillescu, H., Ed.; VCH: Weinheim, 1991.
(2) Prud'homme, J.; Perrier, M.; Denault, J. *Macromolecules* **1994**, *27*, 1493.
(3) Hoffmann, A.; Koch, T.; Stühn, B. *Macromolecules* **1993**, *26*, 7288.
(4) Vogt, S.; Gerharz, B.; Fischer, E. W.; Fytas, G. *Macromolecules* **1992**, *25*, 5986.
(5) Yao, M.-L.; Watanabe, H.; Adachi, K.; Kotaka, T. *Macromolecules* **1991**, *24*, 2955.
(6) Molau, G. E. In *Colloidal and Morphological Behavior of Block Copolymers*; Molau, G. E., Ed.; Plenum Press: New York, 1971.
(7) Bradford, E. B.; McKeever, L. D. *Prog. Polym. Sci.* **1971**, *3*, 109.
(8) Hasegawa, H.; Tanaka, H.; Yamasaki, K.; Hashimoto, T. *Macromolecules* **1987**, *20*, 1651.
(9) Woodward, A. E. *Atlas of Polymer Morphology*; Hanser Publisher: New York, 1988; Chapter 4.
(10) Quirk, R. P.; Kinning, D. J.; Fetters, L. J. In *Comprehensive Polymer Science 7*; Allen, G., Ed.; Pergamon Press: Oxford, U.K., 1989.
(11) Thomas, E. L.; Alward, D. B.; Kinning, D. J.; Martin, D. C.; Handline, D. L., Jr.; Fetters, L. J. *Macromolecules* **1989**, *19*, 2197.
(12) Bates, F. S.; Fredrickson, G. H. *Annu. Rev. Phys. Chem.* **1990**, *41*, 525.
(13) Auschra, C.; Stadler, R. *Macromolecules* **1993**, *26*, 2171.
(14) Beckmann, J.; Auschra, C.; Stadler, R. *Macromol. Rapid Commun.* **1994**, *15*, 67.
(15) Balsara, N. P.; Hammouda, B. *Phys. Rev. Lett.* **1994**, *72*, 360.
(16) Koppi, K. A.; Tirrell, M.; Bates, F. S. *Phys. Rev. Lett.* **1993**, *70*, 1449.
(17) Zhang, Y.; Wiesner, U.; Spiess, H. W. *Macromolecules* **1995**, *28*, 778.
(18) Ehlich, D.; Takenaka, M.; Okamoto, S.; Hashimoto, T. *Macromolecules* **1993**, *26*, 189.
(19) Dalvi, M. C.; Lodge, T. P. *Macromolecules* **1993**, *26*, 859.
(20) Coutandin, J.; Sillescu, H.; Voelkel, R. *Makromol. Chem., Rapid Commun.* **1982**, *3*, 649.
(21) Sillescu, H.; Ehlich, D. In *Laser in Polymer Science and Technology: Applications*; Fouassier, J. P., Rabek, J. F., Eds.; CRS Press: Boca Raton, FL, 1990; Vol. III, p 211.
(22) Ehlich, D.; Sillescu, H. *Macromolecules* **1990**, *23*, 1600.
(23) Hashimoto, T.; Shibayama, M.; Kawai, H. *Macromolecules* **1980**, *13*, 1237.
(24) Herrmann, H.; Lüttke, W. *Chem. Ber.* **1968**, *101*, 1708.
(25) Acheson, R. M.; Barltrop, J. A.; Hichens, M.; Hichens, R. E. *J. Chem. Soc., London* **1961**, 650.
(26) Baro, J. Dissertation, Universität Göttingen, 1987.
(27) Antonietti, M.; Coutandin, J.; Grütter, R.; Sillescu, H. *Macromolecules* **1984**, *17*, 798.
(28) Williams, G.; Watts, D. C. *Trans. Faraday Soc.* **1970**, *66*, 80.
(29) Fleischer, G.; Holstein, P. *Acta Polym.* **1984**, *35*, 738.
(30) Ferry, J. D. *Viscoelastic Properties of Polymers*; John Wiley: New York, 1980.
(31) Fujita, H. *Fortschr. Hochpol. Forsch.* **1961**, *3*, 1.
(32) Vrentas, J. S.; Liu, H. T.; Duda, J. L. *J. Appl. Polym. Sci.* **1980**, *25*, 1297.
(33) Vrentas, J. S.; Duda, J. L.; Ling, H.-C. *J. Polym. Sci. Phys.* **1985**, *23*, 275.
(34) Vrentas, J. S.; Duda, J. L.; Ling, H.-C.; Hou, A. C. *J. Polym. Sci. Phys.* **1985**, *23*, 289.
(35) Vrentas, J. S.; Duda, J. L.; Hou, A. C. *J. Polym. Sci. Phys.* **1985**, *23*, 2469.
(36) Stühn, B.; Mutter, R.; Albrecht, T. *Europhys. Lett.* **1992**, *18*, 427.
(37) Rosedale, J. H.; Bates, F. S. *Macromolecules* **1990**, *23*, 2329.
(38) Rein, D. H.; Baddour, R. F.; Cohen, R. E. *J. Appl. Polym. Sci.* **1992**, *45*, 1223.
(39) Csernica, J.; Baddour, R. F.; Cohen, R. E. *Macromolecules* **1989**, *22*, 1493.
(40) Kinning, D. J.; Thomas, E. L.; Ottino, J. M. *Macromolecules* **1987**, *20*, 1129.
(41) Risken, H. *The Fokker-Planck Equation*, 2nd ed.; Springer Verlag: Berlin, 1989.
(42) Doi, M.; Edwards, S. F. *The Theory of Polymer Dynamics*; Clarendon Press: Oxford, U.K., 1986.

MA950396C